Modelling of self-driven particles: foraging ants and pedestrians

Katsuhiro Nishinari

Department of Aeronautics and Astronautics, University of Tokyo, Bunkyo-ku, Tokyo 113-8656, Japan

Ken Sugawara

Department of Information Science, Tohoku Gakuin University, Sendai, 981-3193, Japan

Toshiya Kazama

Department of Computational Intelligence and Systems Science, Tokyo Institute of Technology, meguro-ku, Tokyo 152-8552, Japan

Andreas Schadschneider

Institut für Theoretische Physik, Universität zu Köln D-50937 Köln, Germany

Debashish Chowdhury

Department of Physics, Indian Institute of Technology, Kanpur 208016, India

Abstract

Models for the behavior of ants and pedestrians are studied in an unified way in this paper. Each ant follows pheromone put by preceding ants, hence creating a trail on the ground, while pedestrians also try to follow others in a crowd for efficient and safe walking. These following behaviors are incorporated in our stochastic models by using only local update rules for computational efficiency. It is demonstrated that the ant trail model shows an unusual non-monotonic dependence of the average speed of the ants on their density, which can be well analyzed by the zero-range process. We also show that this anomalous behavior is clearly observed in an experiment of multiple robots. Next, the relation between the ant trail model and the floor field model for studying evacuation dynamics of pedestrians is discussed. The latter is regarded as a two-dimensional generalization of the ant trail model, where the pheromone is replaced by footprints. It is shown from simulations that small perturbations to pedestrians will sometimes avoid congestion and hence allow safe evacuation.

Preprint submitted to Elsevier Science *6 February 2008*

Key words: ants, flow-density relation, cellular automaton, pedestrian, evacuation

1 Introduction

Modelling of self-driven particles is a recently progressing research area in physics, and opens a new paradigm in statistical physics [1,2]. Self-driven particles, such as vehicles, pedestrian and ants, do not necessarily satisfy Newton's third law, i.e., the law of action and reaction. This is mainly because the force acting among such particles has a psychological or social origin, and hence the reaction differs from one individual to another. Therefore the behavior of these particles is not well described by the usual framework of mechanics or (equilibrium) statistical physics. Nevertheless in the case of collective motion, some aspects of the behavior have similarities with those seen in Newtonian particles, such as phase transitions, cluster formation and occurrence of domain walls [1,2].

There are several attempts to describe such self-driven particles for the last several decades, ranging from differential equations with some social forces [3,4], to cellular automaton (CA) models with various update rules [5,2]. In this paper, we show modellings of ants and pedestrians by a cellular automaton approach in an unified way. We demonstrate similarities between ants on a trail and pedestrians in evacuations, since both try to follow others through sniffing pheromone on a trail, and information from one's eyes and ears, respectively. The behavior of pedestrians is usually not simple in normal situations, but in emergency cases like evacuation from a building on fire, people rush to exits and only simple motions are observed. In this paper we restrict ourselves to the case of evacuation in the modelling of pedestrians. For this case, we show that human behavior can be modeled by a naturally extended model of ants.

The paper is organized as follows. In Sec. 2, we introduce our model of traffic of ants on a trail, and discuss its dynamical properties such as loose cluster formation and anomalous flow-density relation by using a solvable stochastic model. We have also performed an experiment on our ant trail model by developing a multiple robots system. In Sec. 3, a stochastic model of pedestrian dynamics is presented, which is called the *floor field* model. We discuss the relation of the floor field model and the ant trail model, and show simulated results of the model by taking into account the inertia of pedestrians. Concluding remarks and future problems are given in Sec. 4.

2 Traffic of ants

2.1 Ant trail model

Let us first define the ant trail model (ATM) which is a simple model for an unidirectional motion of ants on a trail. The ants communicate with each other by dropping a chemical called *pheromone* on the substrate as they move forward [6]. The pheromone sticks to the substrate long enough for the other following ants to pick up its smell and follow the trail.

First we divide the one-dimensional trail into L cells, each of which can accommodate at most one ant at a time. We will use periodic boundary conditions, that is, we consider an ant trail of a circuit type. The lattice cells are labeled by the index i ($i = 1, 2, ..., L$), and we associate two binary variables S_i and σ_i with each site i. S_i takes the value 0 or 1 depending on whether the cell is empty or occupied by an ant. Similarly, $\sigma_i = 1$ if the cell i contains pheromone; otherwise, $\sigma_i = 0$. Since a unidirectional motion is assumed, ants do not move backward in this model. Their hopping probability becomes higher if it smells pheromone ahead of it. The state of the system is updated at each time step in two stages. In stage I, ants are allowed to move, and stage II corresponds to the evaporation of pheromone. In each stage the dynamical rules are applied in parallel to all ants and pheromones, respectively.

Stage I: Motion of ants

An ant at cell i that has an empty cell in front of it, i.e., $S_i(t) = 1$ and $S_{i+1}(t) = 0$, hops forward with probability Q if $\sigma_{i+1}(t) = 1$ and q if $\sigma_{i+1}(t) = 0$. Here we assume $q < Q$ for consistency with real ant-trails where pheromone works as an attractive chemical for ants on a trail.

Stage II: Evaporation of pheromones

At each cell i occupied by an ant after stage I a pheromone will be created, i.e., $\sigma_i(t+1) = 1$ if $S_i(t+1) = 1$. On the other hand, any free pheromone at a site i not occupied by an ant will evaporate with the probability f per unit time, i.e., if $S_i(t+1) = 0$, $\sigma_i(t) = 1$, then $\sigma_i(t+1) = 0$ with probability f and $\sigma_i(t+1) = 1$ with probability $1 - f$.

The rules can be written in a compact form as the following coupled equations:

$$S_j(t+1) = S_j(t) + \min(\eta_{j-1}(t), S_{j-1}(t), 1 - S_j(t)) - \min(\eta_j(t), S_j(t), 1 - S_{j+1}(t)), \quad (1)$$

$$\sigma_j(t+1) = \max(S_j(t+1), \min(\sigma_j(t), \xi_j(t))), \quad (2)$$

where ξ and η are stochastic variables defined by $\xi_j(t) = 0$ with probability f and $\xi_j(t) = 1$ with probability $1 - f$, and $\eta_j(t) = 1$ with probability $p = q + (Q - q)\sigma_{j+1}(t)$ and $\eta_j(t) = 0$ with probability $1 - p$. We point out that eqs. (1) and (2) reduce to the asymmetric simple exclusion process (ASEP) [7], which is one of the exactly solvable models, if p is a constant, i.e., p does not depend on σ. If we further consider the deterministic limit $p = 1$, then this model reduces to the Burgers CA [8], which is also exactly solvable.

2.2 Numerical results

The ASEP with parallel updating has been used often as a simple model of vehicular traffic on single-lane highways [5]. The most important quantity of interest in the context of flow properties of the traffic models is the *fundamental diagram*, i.e., the flow-versus-density relation, where flow is the product of the density ρ and the average speed V. Thus it is interesting to compare the fundamental diagram of the ATM with that for vehicular traffic.

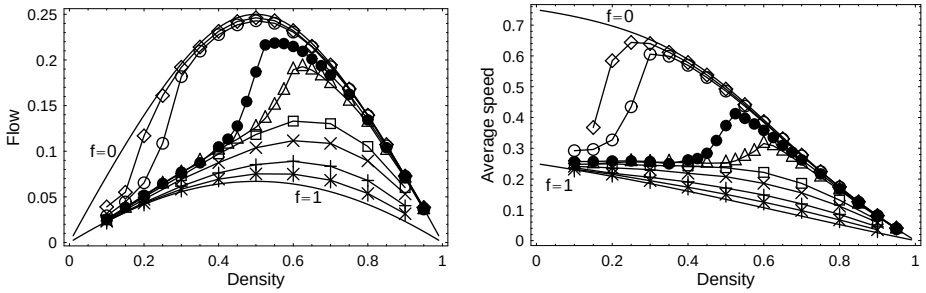

Fig. 1. The average flow (a), speed (b) of the ants are plotted against their densities for the parameters $Q = 0.75, q = 0.25$ and $L = 500$. The discrete data points correspond to $f = 0.0005(\diamond)$, $0.001(\circ)$, $0.005(\bullet)$, $0.01(\triangle)$, $0.05(\square)$, $0.10(\times)$, $0.25(+)$, $0.50(*)$. The cases $f = 0$ and $f = 1$ are also displayed, which are identical to the ASEP corresponding to the effective hopping probabilities Q and q, respectively.

Numerical results of the fundamental diagrams of the ATM is given in Fig. 1(a). The density-dependence of the average speed of the ATM is also shown in Fig. 1(b). We first observe that the diagram does not possess particle-hole symmetry. In the ASEP the flow remains invariant under the interchange of ρ and $1 - \rho$; this particle-hole symmetry leads to a fundamental diagram that is symmetrical about $\rho = \frac{1}{2}$. In the ATM, particle-hole symmetry is seen in the special cases of $f = 0$ and $f = 1$ from Fig. 1(a). In these two special cases the ant-trail model becomes identical to the ASEP with parallel updating corresponding to the effective hopping probabilities Q (for $f = 0$) and q (for $f = 1$), respectively.

Next, over a range of small values of f, it exhibits an anomalous behavior

in the sense that, unlike common vehicular traffic, V is not a monotonically decreasing function of the density ρ (Fig. 1(b)). Instead a relatively sharp crossover can be observed where the speed *increases* with the density. In the usual form of the fundamental diagram (flow vs. density) this transition leads to the existence of an inflection point (Fig. 1(a)).

By a detailed study of the spatio-temporal behavior in the steady-state, we were able to distinguish three different density regimes [9]. At low densities a loosely assembled cluster is formed and propagates with the probability q (Fig. 2). The leading ant in the cluster which hops with probability q will determine the velocity of the cluster. Homogeneous mean field theories fail in this region since these theories always assume that ants are uniformly distributed, which is not true in the case of the ATM [9].

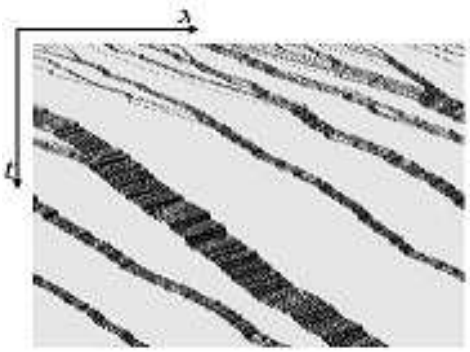

Fig. 2. Spatial-temporal behaviors of loose clusters in the low density case ($\rho = 0.16$). Parameters are $Q = 0.75, q = 0.25, f = 0.005$. We see the loose clusters emerge from the random initial configuration, which will eventually merge after sufficiently long time into one big loose cluster.

In the intermediate density regime, the leading ant occasionally hops with probability Q instead of q, because it becomes possible to feel the pheromone which is dropped by the last ant in the preceding cluster. This arises from the fact that, due to the periodic boundary conditions, the gap size between the last and leading ant becomes shorter as the cluster becomes larger, so that the leading ant is likely to find the pheromone in front of it. This increase of the average speed in this intermediate-density region (Fig. 1(b)), leads to the anomalous fundamental diagram.

Finally, at high densities, the mutual hindrance of the ants dominates the flow behavior leading to a homogeneous state similar to that of the ASEP. In this regime the loose cluster does no longer exist and ants are uniformly distributed after a long time. Thus homogeneous mean field theories give a good result in accounting the fundamental diagram only in this regime [9].

2.3 Analytical results

The ATM is closely related to the zero-range process (ZRP), which is known as one of the exactly solvable models of interacting Markov processes [10,11]. The ZRP consists of the moving particles of the exclusion process. The hopping probability of a particle depends on the number of cells to the particle in front. Hence the ZRP is regarded as a generalization of ASEP. In the ATM, the hopping probability u can be expressed as

$$u = q(1-g) + Qg, \tag{3}$$

where $g(x) = (1-f)^{x/V}$ (Fig. 3). Assuming that a gap size of successive ants is x, g represents the probability that there is a surviving pheromone on the first site of a gap [12]. Thus, since in the ATM the hopping probability u is

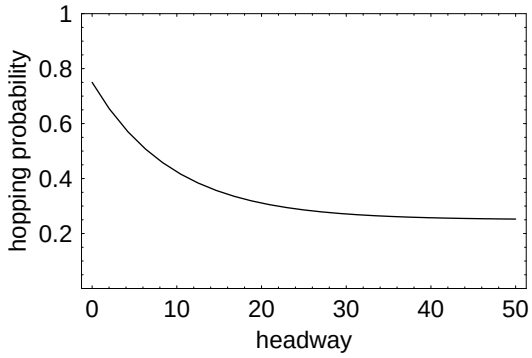

Fig. 3. Hopping probability versus the number of cells between successive ants. Parameters are $Q = 0.75, q = 0.25, f = 0.1$ and $V = 1$ in (3).

related to x, we may utilize the exact results for the ZRP [11]. The average velocity V of ants is then calculated by

$$V = \sum_{x=1}^{L-M} u(x)p(x) \tag{4}$$

where L and M are the system size and the number of ants respectively (hence $\rho = M/L$ is the density), and $p(x)$ is the probability of finding a gap of size x, which is given by

$$p(x) = h(x)\frac{Z(L-x-1, M-1)}{Z(L,M)}. \tag{5}$$

Since the ATM is formulated with parallel update, the form of $h(x)$, as calculated in (5), is given by [13]

$$h(x) = \begin{cases} 1 - u(1) & \text{for} \quad x = 0 \\ \dfrac{1-u(1)}{1-u(x)} \displaystyle\prod_{y=1}^{x} \dfrac{1-u(y)}{u(y)} & \text{for} \quad x > 0 \ . \end{cases} \tag{6}$$

The partition function Z is obtained by the recurrence relation

$$Z(L, M) = \sum_{x=0}^{L-M} Z(L - x - 1, M - 1)h(x), \tag{7}$$

with $Z(x, 1) = h(x - 1)$ and $Z(x, x) = \{h(0)\}^x$, which is easily obtained by (5) with the normalization $\sum p(x) = 1$.

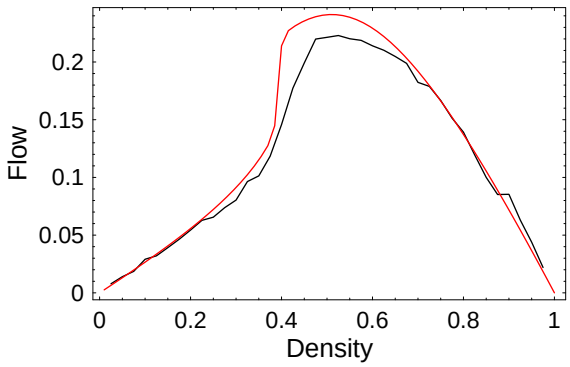

Fig. 4. The fundamental diagram of the ATM with the parameter $L = 200$. Parameters are $Q = 0.75, q = 0.25, f = 0.005$. The smooth thin curve is the theoretical one, while the zigzaged thick one is the numerical data.

Next we draw the fundamental diagram of the ATM by using (4) and changing ρ from 0 to 1. It is given in Fig. 4 with $L = 200$. The thick black curve is the numerical data and the smooth thin black one is the theoretical curve in each figure with the specified value of L. We see that the theoretical curves are almost identical to the numerical ones, thus confirming that the steady state of the ATM is described by the ZRP.

2.4 Multiple robots experiment

Next we set up an experimental system of our ant model by using multiple robots that can communicate with each other through pheromone-like interaction. In this experiment, a virtual pheromone system (V-DEAR) [14] was introduced, in which chemical signals are mimicked by the graphics projected

on the floor, and the robots decide their action depending on the color information of the graphics.

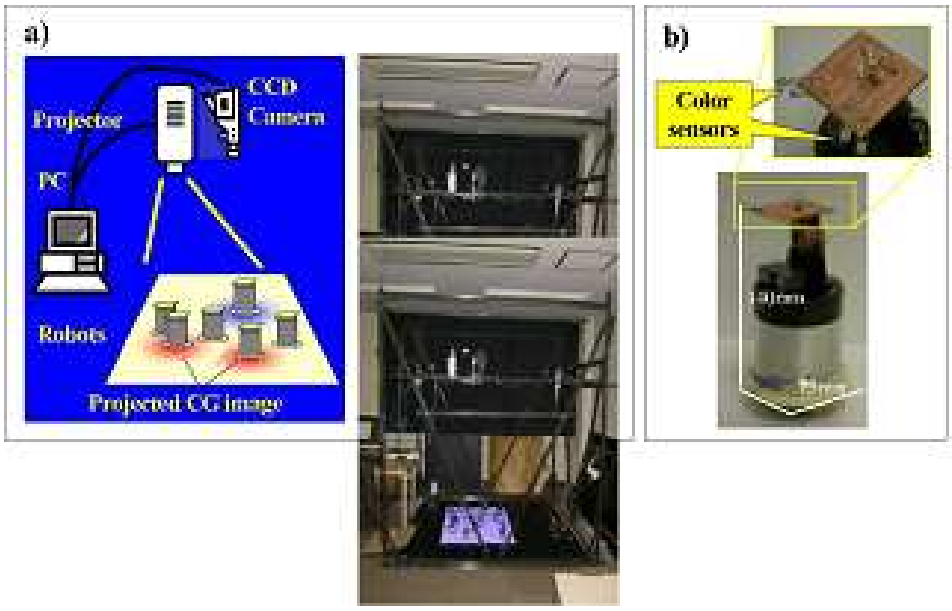

Fig. 5. A schematic view and photo of V-DEAR. (a) The system is composed of Liquid Crystal Projector to project the Computer Graphics and the CCD camera to trace the position of the robots in the field. (b) Each robot has sensors on the top to detect the color and brightness of the field.

Fig. 5 shows the schematic and photo of V-DEAR. Each robot moving on the field detects the color and brightness of the field from sensors on the top, and determines its actions autonomously based on the conditions of the Computer Graphics (CG) on the floor. Combining the position information of the robots acquired from the CCD camera and the projected CG by the projector, we can achieve the dynamic interaction between the environment and robots.

Each robot leaving a pheromone moves in the same direction on the circumference of a circle with diameter 520 mm (Fig. 6, left). The robot immediately behind it traces the pheromone, hence it follows the leader. The speed of each robot $v(x)$ is given by

$$v(x) = \begin{cases} V_Q & \text{for } p(x,t) \geq p_{\text{th}} \\ V_q & \text{for } p(x,t) < p_{\text{th}} \end{cases} \tag{8}$$

where x is the position on the circumference, $p(x,t)$ is the concentration of pheromone at the position and p_{th} is a constant (Fig. 6, middle). If a robot catches up with the robot in front, then the robot in the rear stops moving for 1 sec (Fig. 6, right).

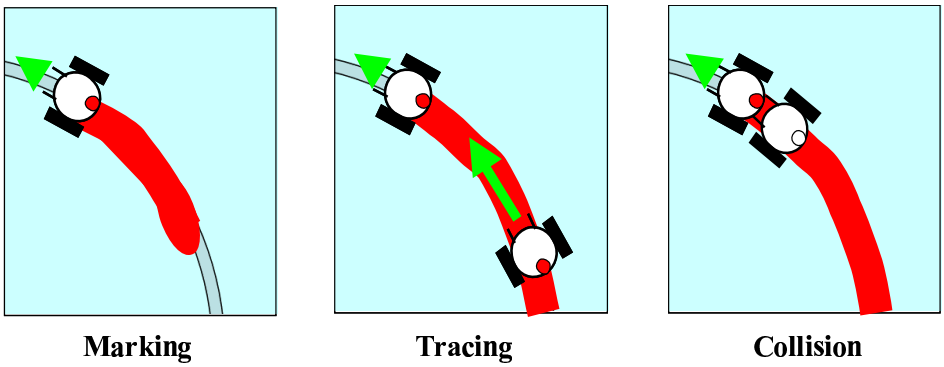

Fig. 6. Interactions between robots through the color CG projected on the floor. Marking, tracing and collision are schematically depicted.

The dynamics of the virtual pheromone is described as

$$\frac{dp(x,t)}{dt} = P - fp(x,t), \tag{9}$$

where f is the rate of evaporation and P the injection concentration given by $P = P_0$ if a robot exists at x, and $P = 0$ if not. $p(x,t)$ is expressed by the gradation of the white color CG which ranges from 0 to 255. In this experiment, we set $V_Q = 7$ cm/s, $V_q = 1.4$ cm/s, $p_{\rm th} = 127$, and $P_0 = 250$.

The experiment was carried out with groups of 4 to 17 robot teams, with $f = 0$, 0.03, 0.05 and 1.00. All experiments were performed one time and had a duration of 3 minutes. As initial condition, robots were distributed evenly on the circle.

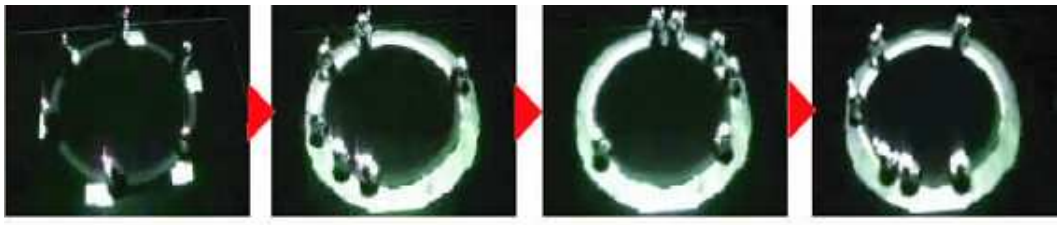

Fig. 7. Loose cluster formation by six robots on a circle.

Fig. 7 shows an example of loose cluster formation of robots in this experiment. The maximal group size of robots on the circumference is 22, hence Fig. 7 corresponds to a density of 6/22. Flow is defined as the number of robots crossing a fixed point on the circumference during the experimental

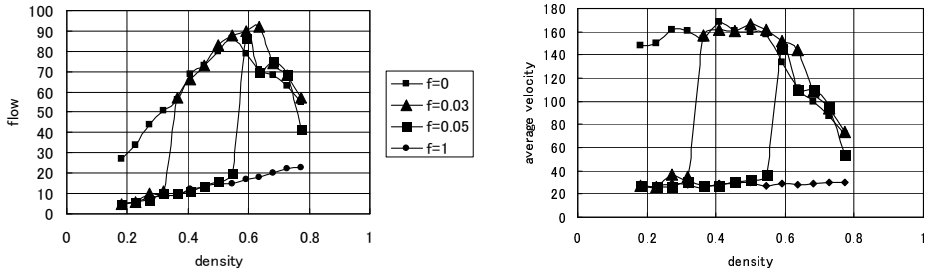

Fig. 8. Fundamental diagram of the robots experiments for $f = 0, 0.03, 0.05$ and 1. We see that the velocity increases sharply for the small but finite values of f, which is similar to fig.1.

duration. The fundamental diagram of our experiment is given in Fig. 8. It shows anomalous features very similar to Fig. 1, although the robot experiment is subject to various perturbations. From Fig. 8 the average velocity surely increases only in the small f cases. Thus we confirm in this experiment that our finding on the anomalous behavior in the ATM is robust and may happen in nature if the evaporation rate of pheromone is sufficiently low.

3 Modelling of evacuations

3.1 Floor field model

We consider a model for pedestrians in evacuation in this section by using a cellular automaton approach. The model is called the floor field model [15] (FFM), which is successfully used up to now for modelling panic behavior of people evacuating from a room. The two-dimensional space is discretized into cells of size 40 cm $\times$ 40 cm which can either be empty or occupied by one pedestrian. Each pedestrian can move to one of the unoccupied Neumann-neighbor cells (i, j) or stay at the present cell at each time step $t \to t + 1$ according to certain transition probabilities p_{ij} as explained below. The important step for this model is to introduce two kinds of floor fields: The *static floor field* S describes the shortest distance to an exit door. The field strength S_{ij} is set inversely proportional to the distance from the door. The other one is the *dynamic floor field* D, which is a virtual trace left by the pedestrians similar to the pheromone in chemotaxis. It has its own dynamics, namely diffusion and decay, which leads to broadening, dilution and finally vanishing of the trace.

The update rules of the FFM have the following structure:

(1) The dynamic floor field D is modified according to its diffusion and decay

rules, controlled by the parameters α and δ.

(2) For each pedestrian, the transition probabilities p_{ij} for a move to an unoccupied neighbor cell (i, j) are determined by the two floor fields. The values of the fields D (dynamic) and S (static) are weighted with two sensitivity parameters k_D and k_S:

$$p_{ij} \sim \exp(k_D D_{ij}) \exp(k_S S_{ij}) P_I(i,j) \xi_{ij}. \tag{10}$$

Here P_I represents the inertia effect [16] given by $P_I(i,j) = \exp(k_I)$ for the direction of one's motion in the previous time step, and $P_I(i,j) = 1$ for other cells, where k_I is the sensitivity parameter. ξ_{ij} is responsible for the exclusion in a cell; if the target cell is occupied by another pedestrian or an obstacle, then we set $\xi_{ij} = 0$, while $\xi_{ij} = 1$ if it is free.

(3) Each pedestrian chooses randomly a target cell based on the transition probabilities p_{ij} determined by (10).

(4) Whenever two or more pedestrians attempt to move to the same target cell, the movement of *all* involved particles is denied with probability $\mu \in [0, 1]$, i.e. all pedestrians remain at their site. Which one is allowed to move is decided using a probabilistic method [17].

(5) The pedestrians who are allowed to move perform their motion to the target cell chosen in step 3. D at the origin cell (i, j) of each *moving* particle is increased by one: $D_{ij} \to D_{ij} + 1$.

The above rules are applied to all pedestrians at the same time (parallel update).

Let us now briefly explain the similarities between the FFM and the ATM. Considering a one-dimensional variant of the FFM, the hopping probability (10) of moving forward for a pedestrian at cell i is simply written as $p_i \sim \exp(k_D D_{i+1})$, where D_{i+1} is the number of footprints at the next cell $i + 1$. Here assuming a unidirectional motion of pedestrians, the static floor field and inertia can be omitted in (10). Thus the FFM takes into account the concentration of multiple pheromones, i.e., footprints at a cell. In the ATM, p_i takes only two values, Q and q, depending on $D_{i+1} = 1$ or 0 respectively. Thus if we restrict the binary values for D as $D \to \min(1, D)$, then the one-dimensional FFM directly corresponds to the ATM if we choose the hopping probability as

$$p_i = q \exp(k_D \min(1, D_{i+1})) \tag{11}$$

where $k_D = \ln Q/q$.

3.2 Model parameters and their physical relevance

There are several parameters in the FFM which are listed below with their physical meanings.

(1) $k_S \in [0, \infty) \cdots$ The coupling to the static field characterizes the knowledge of the shortest path to the doors, or the tendency to minimize the costs due to deviation from a planned route.
(2) $k_D \in [0, \infty) \cdots$ The coupling to the dynamic field characterizes the tendency to follow other people in motion (*herding behavior*). The ratio k_D/k_S may be interpreted as the degree of panic. It is known that people try to follow others particularly in panic situations [3].
(3) $k_I \in [0, \infty) \cdots$ This parameter determines the strength of inertia which suppresses quick changes of the direction of motion. It also reflects the individual's tendency to avoid unnecessary acceleration of the speed during walking.
(4) $\mu \in [0, 1] \cdots$ The friction parameter controls the resolution of conflicts in clogging situations. Both cooperative and competitive behavior at a bottleneck are well described by adjusting μ [18].
(5) $\alpha, \delta \in [0, 1] \cdots$ These constants control diffusion and decay of the dynamic floor field. It reflects the randomness of people's movement and the visible range of a person, respectively. If the room is full of smoke, then δ takes large value due to the reduced visibility.

3.3 Simulations

We focus on measuring the total evacuation time by changing the parameter k_I. The size of the room is set to 100×100 cells. Pedestrians try to keep their preferred velocity and direction as long as possible for minimizing their effort. This is taken into account by adjusting the parameter k_I. In Fig. 9, total evacuation times from a room without any obstacles are shown as function of k_D in the cases $k_I = 0$ and $k_I = 3$. We see that it is monotonously increasing in the case $k_I = 0$. This is because any perturbation from other people becomes large if k_D increases, which causes the deviation from the minimum route. Introduction of inertia effects, however, changes this property qualitatively, and the *minimum* time appears around $k_D = 1$ in the case $k_I = 3$. This is well explained by taking into account the physical meanings of k_I and k_D. If k_I becomes larger, people become less flexible and all of them try to keep their own minimum route to the exit according to the static floor field regardless of congestion. For the (unrealistic) case of very large values of k_I their motion will be completely determined by inertia and thus they might not be able to find the exit at all. By increasing k_D, disturbances from other people become

relevant through the dynamic floor field. This perturbation makes one flexible and hence contributes to avoid congestion, especially at the exit. Large k_D again works as strong perturbation as in the case of $k_I = 0$, which diverts people from the shortest route largely. Note that if we take sufficiently large k_I, then the effect of k_D becomes relatively weak and smooth evacuation will be prevented due to the strong clogging at the exit.

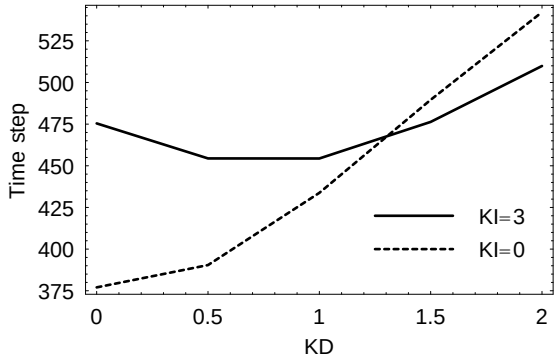

Fig. 9. Total evacuation time vs. coupling k_D to the dynamic floor field for different values of k_I. The room is a simple square without obstacles and 50 simulations are averaged for each data point. Parameters are $\rho = 0.04, k_S = 2$, $\alpha = 0.2$, $\delta = 0.2$ and $\mu = 0$.

4 Conclusion

In this paper, we have studied simple models for ants and pedestrians in an unified way. Ants on a trail follows pheromone dropped by its preceding ants, and pedestrians also follow others in a crowded or panic situation mainly for safe and efficient reasons. We have proposed stochastic cellular automaton models of both ants on a trail and pedestrians in evacuation.

The ant trail model shows an anomalous flow-density relation, which can be analyzed by a ZRP. We have shown that this behavior is also seen in an experiment of multiple robots. It is interesting to see whether the fundamental diagrams remains anomalous when we introduce more then two velocities in (8). Since the velocity of ants in reality allows more gradations, it is important to test how robust the anomaly predicted by the simple model is.

Some generalizations of the ATM have been recently studied: For open boundary conditions, we have a similar phase diagram where the critical point depends on the evaporation probability f [19]. A simple bidirectional generalization is also proposed in [20]. It is interesting to compare the fundamental diagram recently obtained in an experiment with bidirectional leaf-cutting ants [21] with that of the bidirectional model. The FFM can be regarded as a

two-dimensional generalization of the ATM, where the pheromone is replaced by footprints. By using the FFM it is shown that the small perturbation to pedestrians can reduce the total evacuation time in some cases.

Finally, it is interesting to study how a trail of ants between their nest and a food source is created by extending the ATM to two spatial dimension. Then we can directly compare the behaviors of ants and pedestrians by using the two models, and hopefully we will find good strategies of evacuation from the behaviors of ants that have "swarm intelligence" [22].

References

[1] D. Helbing, Rev. Mod. Phys. **73**, 1067 (2001).

[2] D. Chowdhury, L. Santen, and A. Schadschneider, Phys. Rep. **329**, 199 (2000).

[3] D. Helbing, I. Farkas, and T. Vicsek, Nature **407**, 487 (2000).

[4] A. Dussutour, V. Fourcassié, D. Helbing, and J.L. Deneubourg, Nature **428**, 70 (2004).

[5] K. Nagel and M. Schreckenberg, J. Phys. I **2**, 2221 (1992).

[6] A.S. Mikhailova and V. Calenbuhr, *From Cells to Societies* (Springer, Berlin, 2002).

[7] M.R. Evans and R.A. Blythe, Physica A **313**, 110 (2002).

[8] K. Nishinari and D. Takahashi, J. Phys. A: Math. Gen. **31**, 5439 (1998).

[9] K. Nishinari, D. Chowdhury and A. Schadschneider, Phys. Rev. E **67**, 036120 (2003).

[10] F. Spitzer, Advances in Math. **5**, 246 (1970).

[11] M. R. Evans and T. Hanney, J. Phys. A: Math. Gen. **38**, R195 (2005).

[12] D. Chowdhury, V. Guttal, K. Nishinari, and A. Schadschneider, J. Phys. A: Math. Gen. **35**, L573 (2002).

[13] M.R. Evans, J. Phys. A: Math. Gen. **30**, 5669 (1997).

[14] K. Sugawara, T. Kazama and T Watanabe, Proc. of IEEE/RSJ Int. Conf. on Intel. Robots and Sys. (IROS2004) (2004) p. 3074.

[15] C. Burstedde, K. Klauck, A. Schadschneider, and J. Zittartz, Physica A **295**, 507 (2001).

[16] K. Nishinari, A. Kirchner, A. Namazi, and A. Schadschneider, IEICE Trans. Inf. Syst. **E87-D**, 726 (2004).

[17] A. Kirchner, K. Nishinari, and A. Schadschneider, Phys. Rev. E **67**, 056122 (2003).

[18] A. Kirchner, H. Klüpfel, K. Nishinari, A. Schadschneider, and M. Schreckenberg, Physica A **324**, 689 (2003).

[19] A. Kunwar, A. John, K. Nishinari, A. Schadschneider, and D. Chowdhury, J. Phys. Soc. Jpn. **73**, 2979 (2004).

[20] A. John, A. Schadschneider, D. Chowdhury, and K.Nishinari, J. Theor. Biol. **231**, 279 (2004).

[21] M. Burd, D. Archer, N. Aranwela, and D.J. Stradling, American Natur. **159**, 283 (2002).

[22] E. Bonabeau, M. Dorigo, and G. Theraulaz, *Swarm Intelligence: From Natural to Artificial Systems*, (Oxford University Press, 1999).